BASIC SCIENCE

Reconstruction of orbital defects by implantation of antigen-free bovine cancellous bone scaffold combined with bone marrow mesenchymal stem cells in rats

Jingjing Zhao · Chunbo Yang · Chang Su · Min Yu · Xiaomin Zhang · Shuo Huang · Gang Li · Meili Yu · Xiaorong Li

Abstract

Background Tissue-engineering approach can result in significant bone regeneration. We aimed to reconstruct the segmental orbital rim defects with antigen-free bovine cancellous bone (BCB) scaffolds combined with bone marrow mesenchymal stem cells (BMSCs) in rats.

Jingjing Zhao and Chunbo Yang contributed equally.

J. Zhao
Tianjin Medical University, 22 Qixiangtai Rd,
Tianjin 300070, The People's Republic of China

J. Zhao · C. Yang · C. Su · X. Zhang · X. Li
Tianjin Medical University Eye Hospital, The College of Optometry,
Tianjin Medical University Eye Institute, 251 Fukang Rd,
Tianjin 300384, The People's Republic of China

M. Yu
School of Public Health, Tianjin Medical University,
Tianjin 300070, The People's Republic of China

S. Huang · G. Li
Stem Cells and Regeneration Program, School of Biomedical
Sciences and Li Ka Shing Institute of Health Sciences,
The Chinese University of Hong Kong, Prince of Wales Hospital,
Shatin, NT, Hong Kong, The People's Republic of China

M. Yu (✉)
Tianjin Third Central Hospital Affiliated to Tianjin Medical
University, Tianjin Key Laboratory of Artificial Cells,
83 Jintang Road,
Tianjin 300170, The People's Republic of China
e-mail: yumeili8@163.com

X. Li (✉)
Tianjin Medical University Eye Hospital, The College of Optometry,
Tianjin Medical University Eye Institute, 251 Fukang Rd,
Tianjin 300384, The People's Republic of China
e-mail: lixiaorong@tijmu.edu.cn

Methods BCB was prepared by degreasing, deproteinization and partly decalcification. BMSCs isolated from green fluorescent protein (GFP) transgenic rats were osteogenically induced and seeded onto BCB scaffolds to construct induced BMSCs/BCB composites. An 8-mm full-thickness defect on the rat inferior-orbit rim was established. Induced BMSCs/BCB composites cultured for 5 days were implanted into the orbital defects as the experimental group. Noninduced BMSCs/BCB group, BCB group and exclusive group were set. General condition, spiral CT, 3D orbital reconstruction, histological and histomorphometric analysis were performed after implantation.

Results BCB presented reticular porous structure. GFP-BMSCs adhering to BCB appeared bright green fluorescence and grew vigorously. Infection and graft dislocation were not observed. In induced BMSCs/BCB group, CT and 3D reconstruction showed perfect orbital repair situation. Histological analysis indicated BCB was mostly biodegraded; newly formed bone and complete synostosis were observed. The percentage of newly formed bone was (57.12 ± 6.28) %. In contrast, more residual BCB, less newly formed bone and nonunion were observed in the noninduced BMSCs/BCB group. Slowly absorbed BCB enwrapped by fibrous connective tissue and a small amount of new bone occurred in BCB group. Fibrous connective tissue appeared in exclusive group.

Conclusions Antigen-free bovine cancellous bone that retains natural bone porous structure and moderate mechanical strength with elimination of antigen is the ideal carrier for mesenchymal stem cells in vitro. BCB combined with BMSCs is a promising composite for tissue engineering, and can effectively reconstruct the orbit rim defects in rats.

Introduction

Orbit not only functions to protect the eyeball and its appendices from injuries and preserve the normal position, but also relates to the cranial fossae as well as paranasal and maxillary sinuses. Because of the thin, weak and irregular-shape structure, orbit is prone to suffer from a variety of fractures occurring alone or accompanied with periorbital bone complex fracture, and orbital defect caused by various reasons usually leads to structural damage, functional abnormality and serious complications. The position, structures and mechanical characteristics of orbit increase the difficulty of ideal repair and reconstruction of orbital defect. Therefore, the reconstruction of orbital defect is a challenging task to orbital plastic surgeons for anatomical structure reconstruction and function recovery.

The materials applied to the repair of orbital defect include autologous bone, allogeneic bone, xenogeneic bone and synthetic materials [1]. Although considered as gold standard for bone defect repair and reconstruction, autologous iliac crest bone graft results in higher incidence of donor site morbidity, neurological complications and deep infection [2]. The applications of allogeneic bone and xenogeneic bone implant are hindered by limited donor resources and immune rejection [3]. Several kind of synthetic scaffolds are applied to the orbital defects, such as hydroxyapatite, titanium mesh, polymeric porous polyethylene, polyglycolic acid and so on. But a variety of shortcomings, including nondegradation, infection and cyst formation, have compromised the therapeutic outcomes [4–9].

Currently, tissue engineering that is different from the conventional therapeutic strategy represents the prominent trend for orbital reconstruction. Furthermore, the tissue engineering strategy for the reconstruction of orbital rim defects should be distinguished from those used for the reconstruction of long bones and mandible bones. The scaffold should be designed according to the complex and respective shape of individuals before the implantation and the non-weight-bearing orbital rims will bear lower stress in the remodeling procedure.

The degradable biomaterial scaffold and seeding cells are critical factors in tissue engineering [10]. In this study, antigen-free bovine cancellous bone (BCB) scaffolds were applied as carriers. BCB is a kind of bio-derived bone material whose potential antigens were excluded through a series of processes, while retaining the osteoconductive properties. The porous microstructure, good biocompatibility and osteoconductivity meet the requirements for tissue engineering. It has been successfully applied for repair and reconstruction of bone defects in orthopedics, stomatology, cranial and maxillofacial surgery [11, 12].

Bone marrow mesenchymal stem cells (BMSCs), having the capability of multipotent differentiation and immunosuppressive properties, were used as appropriate seed cells for cell therapy and tissue engineering [13, 14]. In many previous studies, BMSCs induced with the osteogenic induction medium were cultured onto the scaffolds in vitro, and cell-scaffold composites were transplanted into the defect area to complete the healing of bony tissue.

In the present study, we evaluate the therapeutic effect of BMSCs seeded onto BCB on the repair of orbital rim defects in rats, aiming to explore a more potent strategy for the reconstruction of orbital defects.

Materials and methods

Preparation of antigen-free bovine cancellous bone scaffolds and SEM analysis

The fresh bovine proximal humerus cancellous bone was cut into $8 \times 5 \times 5$ mm^3 and rinsed with water at 70 °C three times. Particles were immersed in 0.5 % Triton X-100 and 10 % sodium chloride to remove cells. After immersion in the mixture of equal volume of methanol and chloroform for 12 h to degrease, they were deproteinized with 30 % hydrogen peroxide for 24 h, which was repeated three times. Then they were dunked in 0.5 M hydrochloric acid for 5 min for partial decalcification. BCB particles were sterilized by Co-60 gamma irradiation and stored at −80 °C. The porosity of BCB was 80 %. The pore diameter of BCB was about 300–500 μm.

Four specimens of BCB particles were crushed to fragments and coated with gold powder, followed by observation by a scanning electron microscopy (S-3500N; Hitachi Ltd, Tokyo, Japan).

Isolation and culture of bone marrow-derived mesenchymal stem cells

All experiments were performed in compliance with the ARVO (Association for Research in Vision and Ophthalmology) statement for the Use of Animals in Ophthalmic and Vision research. BMSCs of green fluorescent protein (GFP)-transgenic rats (SLC Inc., Shizuoka, Japan) were isolated as previously described [15]. Briefly, the femurs of rats were harvested and the bone marrow was flushed out by a syringe filled with 1 ml of low glucose-Dulbecco's modified Eagle's medium (L-DMEM; Gibco, USA) supplemented with 10 % fetal bovine serum (FBS; Gibco, USA). The medium containing cells were layered over Percoll solution ($D=1.073$ g/ml; Biochrom, Berlin, Germany) and centrifuged at 850 g for 25 min. The intermediate lay was suspended in Percoll diluted with an equal volume of PBS following centrifugation at 850 g for 10 min. The cells were

resuspended in 5 mlL-DMEM supplemented with 10 % FBS and seeded in T-25 flasks at a concentration of 2×10^6 cell/ml. Cells were incubated at 37 °C in 5 % CO_2 in a fully humidified air. Nonadherent cells were removed by replacing the medium. The GFP-BMSCs were positive for CD44 and CD90 and negative for CD45 and CD31. Expanded cultures of BMSCs were analyzed for chondrogenic, osteogenic and adipogenic differentiation in vitro to determine multipotency according to standard conditions described previously [16].

Induction of osteogenic differentiation

BMSCs were separated into two parts. Induced BMSCs were prepared as follows: The culture medium was replaced with L-DMEM containing 10 % FBS, 10 nM dexamethasone (Sigma, St. Louis, MO), 10 mM β-glycerophosphate (Sigma, St. Louis, MO) and 50 μg/ml ascorbate-2- phosphate (Sigma, St. Louis, MO) for osteogenic culture. The other half of BMSCs were cultured in L-DMEM containing 10 % FBS to construct noninduced BMSCs. The Osteogenic medium and noninduction medium were changed every 3 days.

Construction of cell-material complex in vitro

BCB particles were rehydrated with L-DMEM containing 10 % FBS at room temperature for 4 h in a 24-well plate. Third-passage BMSCs were suspended in L-DMEM containing 10 % FBS at a density of 2×10^6 cell/ml. Five hundred μl BMSC suspension was dropped into BCB scaffold using a 1 ml syringe fitted with 18-gauge needle in each well, and cells were allowed to attach to scaffolds for 4 h

before 500 μl of osteogenic induction media or noninduction medium was gently added. The complexes were incubated at 37 °C for 5 days. Half of the medium was replaced every 2 days.

Four samples of induced BMSCs/BCB composites, noninduced BMSCs/BCB composites and BCB scaffolds were observed with fluorescence microscopy (BX61; Olympus Optical Co., Tokyo, Japan) before implantation.

Experimental animals and surgical procedure

The experimental protocol was approved by the Experiment Center of Tianjin Medical University. Forty 8-week-old male Sprague-Dawley rats (250–300 g) were anesthetized with an intraperitoneal injection of 10 % chloral hydrate (300 mg/kg). A 1-cm longitudinal incision 2 mm below and parallel to the lower eyelid was made, providing the access to the orbit through the soft tissue (Fig. 1a). An 8 mm full-thick defect in the right inferior orbit rim was manufactured with an electric bone saw. Bone chips and periosteum were removed (Fig. 1b). Rats were divided into four groups randomly, $n=10$ in each group. For the induced BMSCs/BCB group, the broken orbital rims were implanted with induced BMSCs/BCB composites (Fig. 1c); for the noninduced BMSCs/BCB group, they were implanted with noninduced BMSCs/BCB composites; for the BCB group, they were implanted with BCB scaffolds; and for the exclusive group, they were not implanted as negative control. Fascia, muscle and skin were sutured separately and erythromycin ointment was administered twice a day for 5 days (Fig. 1d). All procedures above were under sterile condition.

Fig. 1 The implantation procedure for reconstruction of the inferior orbital rim defect in rat. Exposure of inferior orbit (a). Inferior orbital rim defect modeling (b). BMSCs/BCB composite was implanted into defect area (c). Incisions closure (d)
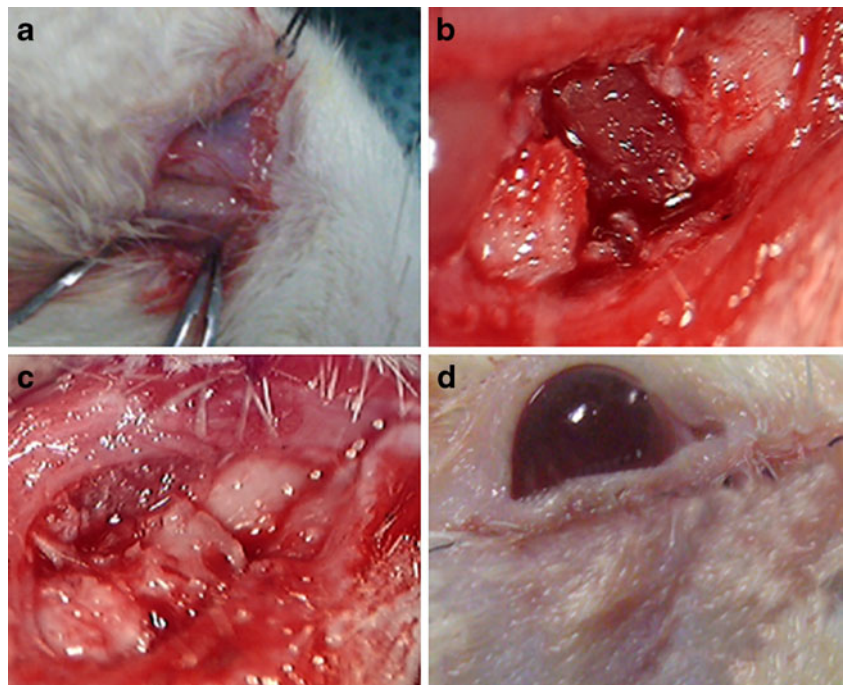
General observation after operation

Food and water intake, activity and incision situation of all rats were observed and recorded daily after operation.

Spiral computed tomography and three-dimensional orbital reconstruction

Spiral CT with a thickness of 0.625 mm was performed with a spiral CT scanner (Somatom Definition, Siemens Healthcare, Forchheim, Germany) and 3D orbital reconstruction with a thickness of 1.25 mm was processed in Workstation (ADW4.1) with UNIX System in DICOM format at 2, 4, 8, 12 weeks after operation.

Histological analysis

Tissue samples of the inferior orbits were harvested at 12 weeks after implantation. One half of the specimens were fixated in 10 % neutral buffered formalin, dehydrated in a graded series of ethanol and soaked in xylene, then embedded in methylmetacrylate. Sections of 7 μm-thickness were prepared and stained with von Kossa/van Gieson. Another half of the specimens were decalcified with 10 % sodium ethylenediamine-tetra-acetate after fixation in 10 % buffered formalin. The samples were processed by graded alcohols and xylene, and embedded with paraffin. Paraffin sections in a thickness of 5 μm were stained with hematoxylin-eosin (H&E).

Histomorphometric analysis

Histomorphometric analysis was performed 12 weeks after implantation. The same longitudinal sections were observed by a video digital camera (Model DXC-930P, Sony, Tokyo, Japan) linked to an image processing system using Image-Pro Plus 4.5 image software (Media Cybernetics, Silver Springs, MD, USA). Five sections from each sample were analyzed and five regions in each section were photographed at 200× magnification. The percentage of newly formed bone area in the total area of the selected region in the defect area was calculated to represent the ability of osteogenesis.

Statistical analysis

All data were presented as mean ± standard deviation (SD). Statistical analysis was evaluated using SPSS14.0 (SPSS Inc., Chicago, Illinois) by the method of one-way analysis of variance. A p-value of less than 0.05 was considered statistically significant for all the analysis.

Result

The structure of BCB scaffolds

The structure of BCB scaffolds presented uniformly distributed, interconnected reticular network (Fig. 2a); SEM analysis showed clear porous structure (Fig. 2b) and trabecular structure (Fig. 2c) of antigen-free bovine cancellous bone scaffolds.

Fluorescence microscopy analysis of cell-material complexes

Figure 3 shows fluorescence microscopy images of BMSCs seeding onto the BCB scaffolds cultured in vitro before implantation. The GFP-BMSCs were distributed uniformly onto the surface of BCB scaffolds in the induced BMSCs/BCB composites (Fig. 3a) and noninduced BMSCs/BCB composites (Fig. 3b), which appeared as bright green fluorescence.

General observation after operation

The diet, activity and eyeball motility of all experimental animals were normal throughout the process after operation in all four groups. Mild swelling around incision areas occurred within 4 days after operation. The healing of the incisions was uneventful without infection, implants dislocation or adverse tissue reactions within the first postoperative week.
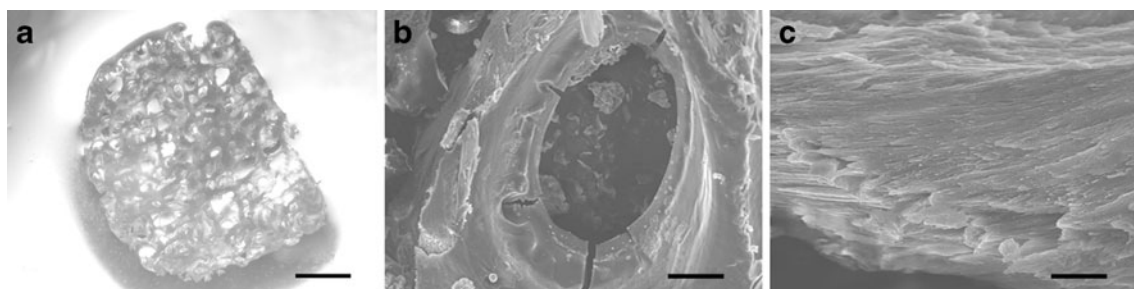
Fig. 2 The images of BCB scaffold. The appearance images showed the interconnected reticular network (**a**). SEM images showed the porous structure (**b**) and trabecular structure of BCB (**c**). Scale bars **a** 1,000 μm. **b** 100 μm. **c** 10 μm

Fig. 3 The images of induced BMSCs/BCB composite, noninduced BMSCs/BCB composite and BCB scaffold 5 days after culture in vitro. With GFP as a marker, BMSCs were evenly distributed on the surface of BCB in induced BMSCs/BCB composite (a) and noninduced BMSCs/BCB composite (b) under fluorescence microscopy. No fluorescence in BCB scaffold without cell seeding(c). Induced BMSCs/BCB composite (d), noninduced BMSCs/BCB composite (e) and BCB without cells (f) under light microscope. Scale bar, 300 μm
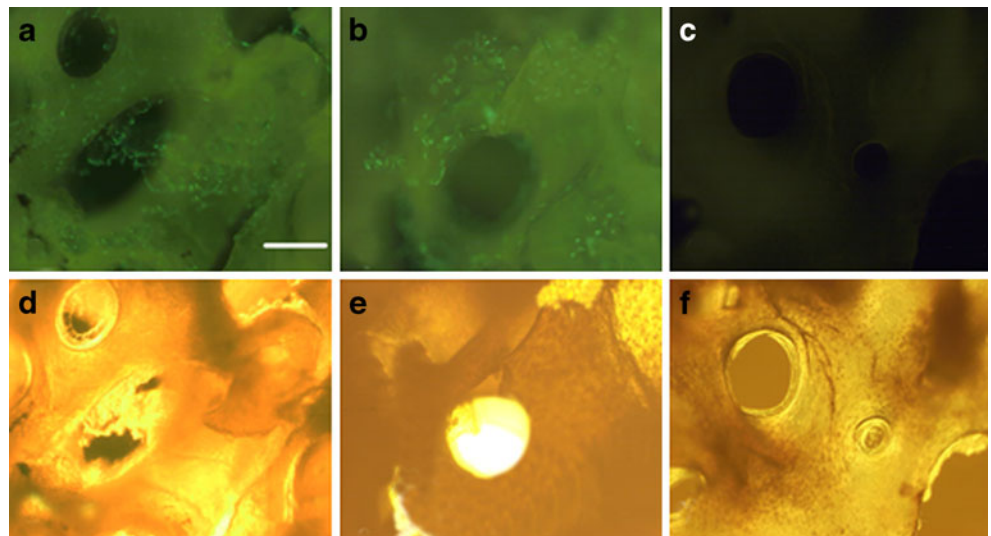

Spiral computed tomography and three-dimensional orbital reconstruction

Spiral CT scanning and 3D orbital reconstruction were performed to examine the configuration and the location of the implants and the healing status of the inferior orbital rim (Fig. 4).

The initial appearances of the implants were preserved and the implants were in the correct position, which fitted close to the broken orbital rim ends with the clear joint lines in induced BMSCs/BCB group (Fig. 4a), noninduced BMSCs/BCB group (Fig. 4b) and BCB group (Fig. 4c) 2 weeks after operation.

Fig. 4 Three-dimensional orbital reconstruction images at 2, 4, 8, and 12 weeks after implantation. Good appearance and bony union in the induced BMSCs/BCB group (a, d, g, j); Partial synostosis in the noninduced BMSCs/BCB group (b, e, h, k); Nonunion in the BCB group (c, f, i, l)
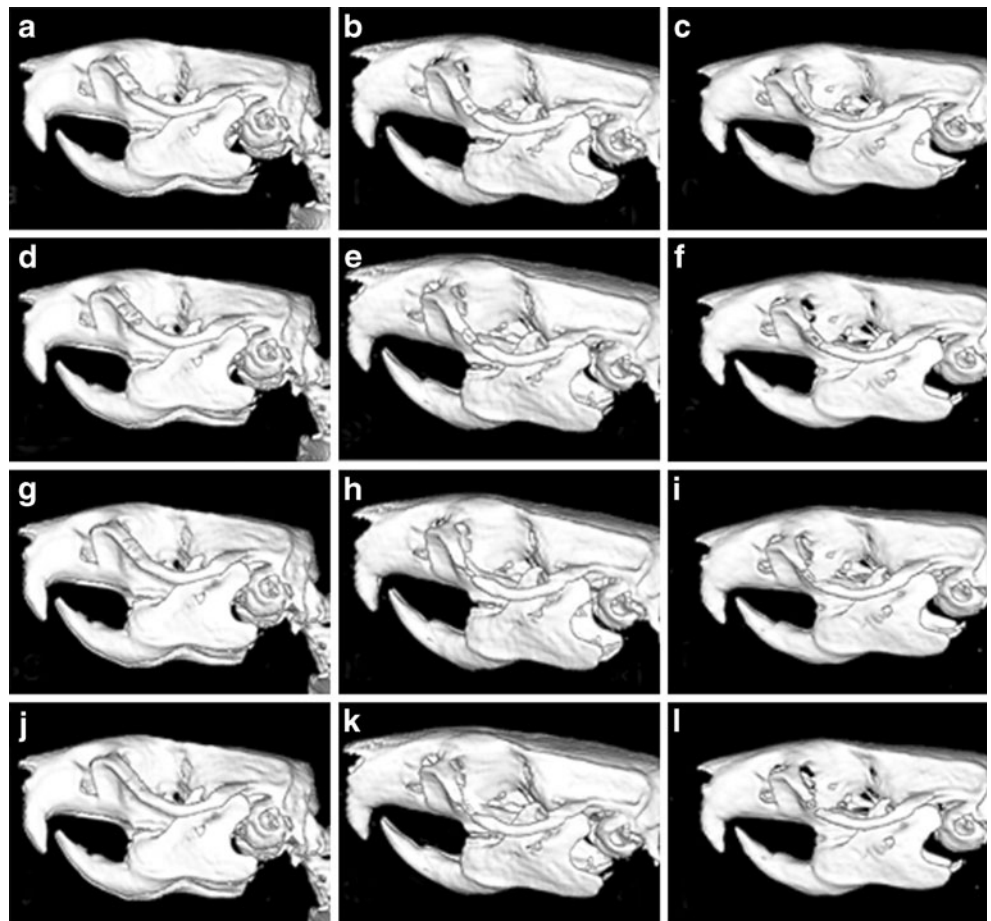
Four weeks after implantation, the implants preserved the initial configuration and repaired the ends with the blurry joint lines in the induced BMSCs/BCB group (Fig. 4d). The implants remained good repair but the legible joint lines in the noninduced BMSCs/BCB group (Fig. 4e). The crevice and the distinct joint lines were observed in the BCB group (Fig. 4f).

Eight weeks after implantation, the inferior orbital rims were reformed while the joint lines were invisible in the induced BMSCs/BCB group (Fig. 4g). The implants diminished in size and the joint lines were obvious in the noninduced BMSC/BCB group (Fig. 4h). The gap expanded and nonunion formed with the obvious joint lines in BCB group (Fig. 4i).

Twelve weeks after implantation, synostosis was observed between the end of the implants and the broken orbital rim ends and the inferior orbital rims were reconstructed entirely in the induced BMSCs/BCB group (Fig. 4j). In the noninduced BMSCs/BCB group, synostosis occurred at the edges of the implants and few ossifications occurred in the center of the implants. So, the inferior orbital rims were not entirely reconstructed (Fig. 4k). Obvious nonunion was observed in BCB group (Fig. 4l).

Histological analysis

The reconstruction process of orbital defect 12 weeks after implantation was assessed by histological analysis. Representative histological images are showed in Fig. 5. Residual BCB scaffolds, lamellar bone, woven bone and fibrous connective tissue were assessed. The residual scaffolds were dissolved during embedding and the blanks were retained as empty holes. Mineralized bone matrix is stained black; non-mineralized osteoid and fibrous connective tissue are stained red in von Kossa/van Gieson staining.

In the induced BMSCs/BCB group, a large amount of newly formed woven bone with irregular bone trabecula surrounded by densely arranged osteoblasts, and a large number of lamellar bone containing the elongated and few osteocytes and orderly arranged collagen fiber bundles were
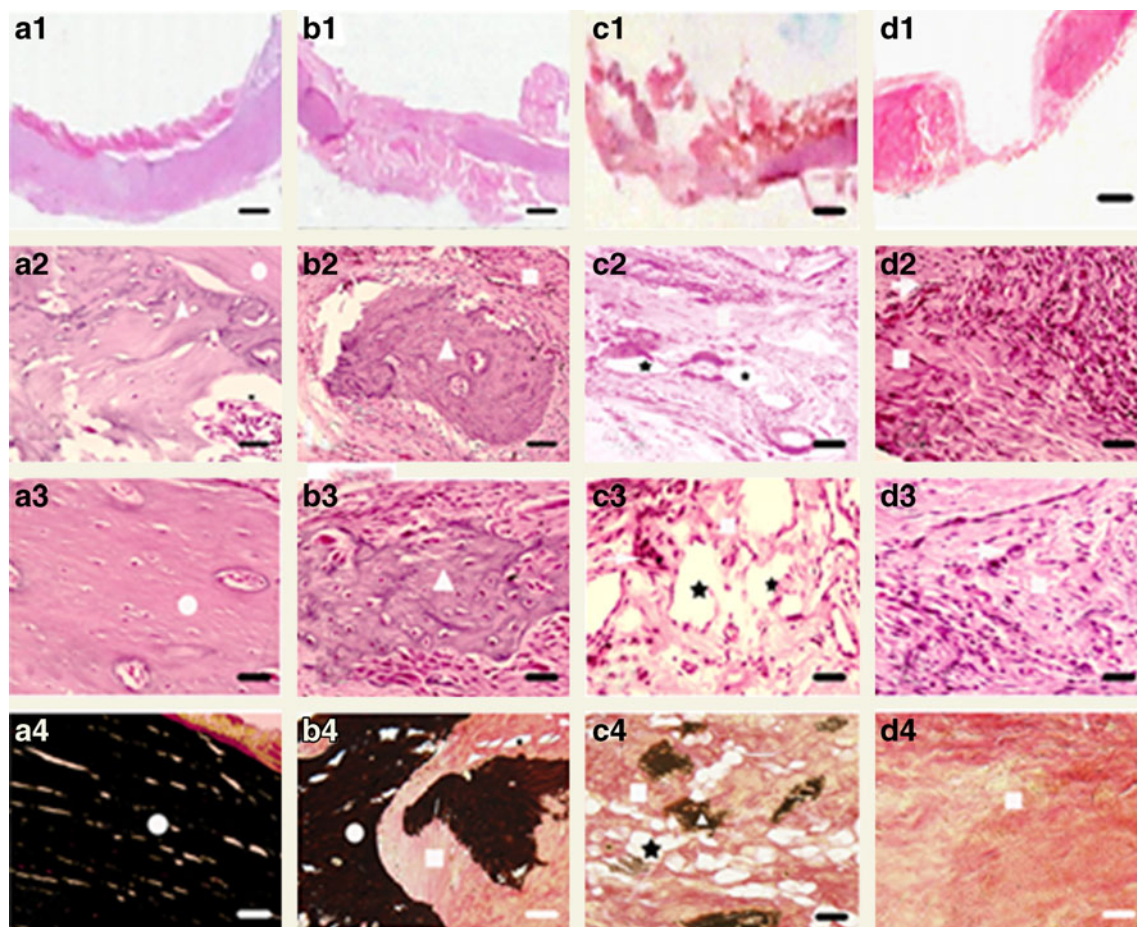
Fig. 5 Histological images at 12 weeks after implantation. Induced BMSCs/BCB group (**a1–a4**); Noninduced BMSCs/BCB group (**b1–b4**); BCB group (**c1–c4**); Exclusive group (**d1–d4**). Scale bars, **a1–d1** 1,000 μm. **a2–d2** 200 μm. **a3–d3** 100 μm. **a4–d4** 200 μm. △-Woven bone; ○-Lamellar bone; →-blood vessel; □-Fibrous connective tissue; ★-The blank areas retained by BCB scaffolds which were dissolved during embedding. **a1–d3** H&E stain. **a4–d4** von Kossa/van Gieson stain

observed. A small amount of BCB particles were dispersed, which indicated that BCB material had been almost completely degraded (Fig. 5a2, a3). A large amount of mineral deposited and complete synostosis appeared between the ends of orbital rim defects and the implants (Fig. 5a4). In the noninduced BMSCs/BCB group, more residual BCB particles and woven bone containing the densely irregular-arranged osteoblasts and inorderly arranged collagen fiber bundles were observed. A certain amount of fibrous tissues appeared in the periphery of woven bone regeneration areas (Fig. 5b2, b3). Few new bone and much fibrous tissue occurred between the ends of orbital rim defects and the implants (Fig. 5b4). In the BCB group, the defects were mostly occupied by fibrous tissue. Few new-forming bone islets and more BCB particles were packed into fibrous tissue (Fig. 5c2–c4). In exclusive group, a large amount of fibrous tissue and the blood vessels were observed and no new bone formed between the broken orbital rim ends (Fig. 5d2–d4).

Histomorphometric analysis

Histomorphometric analysis showed that the percentage of newly formed bone in the areas grafted with induced BMSCs/BCB composite $(57.12\pm6.28)\%$ and noninduced BMSCs/BCB composite $(43.28\pm4.74)\%$ were higher than that in the area grafted with BCB scaffold $(17.21\pm1.62)\%$ at 12 weeks after implantation $(P<0.01)$. There was a statistically significant difference in new bone formation percentage between induced BMSCs/BCB composite and noninduced BMSCs/BCB composite $(P<0.01)$ (Fig. 6).

Discussion

Because of the disadvantages of autograft and allograft, the research of the repair of the orbital defect focuses on the
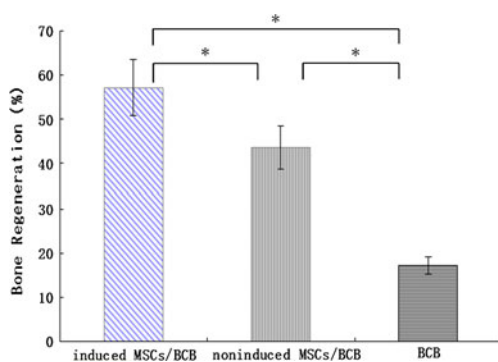
Fig. 6 Bone regeneration percentage of the orbital defect area at 12 weeks after implantation. The induced BMSCs/BCB group showed much a higher bone regeneration rate compared with the noninduced BMSCs/BCB group and the BCB scaffold group. Three bars represent average and error bars represent SD. The asterisks (*) indicate statistically significant differences between different groups $(P<0.01)$

suitable bone-graft substitute. However, some kinds of artificial materials applied in recent years have side effects and shortcomings that have limited their applications. Hydroxyapatite and porous high-density polyethylene lead to dislocation, failure of combination with planting bed and matrix mineralization suppression [4, 5]. Titanium suppresses bone matrix mineralization through induction of apoptosis in MSCs [6]. Polydiaxonone sheets and polyglycolic acid can induce inflammatory response and scar formation [7, 8]. β-tricalcium phosphate (β-TCP) degrades into powders and induces toxic effects [9].

In recent years, tissue engineering for the repair of orbital defects that emphasizes the regeneration instead of filling is a new promising approach as a substitute for autografts and allogeneic bone grafts. The critical elements of tissue engineering, which combine the knowledge and technology of material engineering, stem cells and biological factors, include three parts: seed cells, three-dimensional scaffolds and osteogenesis-inducing factors.

BMSCs presenting prominent bone-forming potential are applied widely in bone tissue engineering as the appropriate source of seed cells. BMSCs can release biologically active factors and promote collateral blood flow development through paracrine mechanisms, which are vital for cell growth and tissue repair [17]. BMSCs transplantation are proved to produce more extracellular matrix, improve glycosaminoglycan production and strongly enhance angiogenesis during the course of fracture healing and bone regeneration [13, 14].

An ideal scaffold is another critical element for tissue engineering. Ideal biomaterial scaffolds imperative for the repair of orbital defect should be three-dimensional structure, biodegradability, biocompatibility, cytokines delivering capability and surface osteoconductivity [10]. The degradable materials as scaffolds applied in bone tissue engineering, such as poly-lactic acid, polyglycolic acid and β-TCP, can damage seeding cells by acidic metabolites and toxic effects [5, 8, 9]. Bio-derived materials derived from natural resource and processed through specific methods are the most predominant candidates as scaffolds for bone tissue engineering [18]. Bovine cancellous bone derived from natural material is commonly used to fill small osseous defects in oral and maxillofacial surgeries [19]. BCB integrated with cells or bioactive molecules can promote new bone growth and accelerate the reconstruction of bone defects through modulation of degradation rate and enhancement of osteoconductivity and osteoinductivity of scaffold. The additional advantages of BCB applied to tissue engineering are abundant sources, low price and convenient storage.

In our study, antigen-free bovine cancellous bone scaffolds combined with BMSCs were implanted into the orbit rim defects and reconstructed the orbits with new-forming bone, which has not been reported previously. It was distinctly proved in our study that BCB retaining the reticular

porous structure showed perfect osteoconductivity and contributed greatly to enhance the ability of new bone formation in vivo. The multitudinous and interconnected pores in BCB can provide the passages for cells, growth factors and blood vessels to migrate and expand, which promote bone growth and skeletal maturation [20].

Pore size is a crucial parameter for porous scaffold. The diameter of pore ranged from 300 to 1,200 μm is efficient in supporting cell migration, proliferation and growth factor transport [21]. Our results showed the pore size of BCB can meet the requirements of tissue engineering.

The application of dexamethasone, ascorbate-2-phosphate and β-glycerophosphate is the routine and optimal method for osteogenic induction, which was also used in our study after the harvesting, isolation and expansion of rat BMSCs. Dexamethasone is essential to osteogenic phenotype expression and the recruitment and differentiation of osteoprogenitor cells in rat BMSC cultures. Ascorbate-2-phosphate contributes to collagen deposition and mineral deposition. β-glycerophosphate supplies organic phosphate ions for bone formation [22].

Consistent with previous reports [23, 24], our results of fluorescence microscopy analysis showed that cells seeding onto the antigen-free bovine cancellous bone adhered to the scaffolds well and grew vigorously, which indicated good cytocompatibility of BCB as a carrier for BMSCs .

No infections, adverse tissue reactions or deaths were observed in rats after BCB scaffold and cell-BCB complexes implantation, which indicated the good histocompatibility of BCB as scaffold in vivo, as reported by other researchers [24]. The potential xenoantigens were removed through the processing steps of degreasing, deprotein and partial decalcification. Furthermore, the immunogenicity and enzyme activity were eliminated by irradiation sterilization and cryogenic storage.

The appropriate biodegradation rate is another important ingredient of scaffold in tissue engineering. As previously reported, β-TCP degrades too rapidly and creates powders to inhibit the growth of seeding cells [9], while hydrophilic PCL biodegrades too slowly and decreases the susceptibility to microbial action [25]. Because the bone structures of mammals were homologous, bovine bone-derived scaffolds derived from bovine bone can be assimilated and degraded gradually by the host during the process of new bone formation. According to our results, BCB scaffolds combined with BMSCs were almost degraded at 12 weeks after implantation, indicating that the degradation rate of BCB scaffolds matched bone formation rate of in the area of orbital defect implanted with induced BMSCs/BCB composites.

The critical size defect (CSD) is defined as "the smallest size intraosseous wound in a particular bone and species of animal that will not heal spontaneously during the lifetime of the animal" [26]. The orbit is the cavity of the calvaria in which the eyeball and its appendages are situated. It has

been reported by Schmitz JP [27] et al. that the critical size defect in the rat calvaria is 8 mm and surgical therapy is necessary for the defect repair. Then many investigators [19, 28] have applied this model in correlative researches. In our study, no new bone formation was observed in the area of the 8 mm full-thickness orbital defect, which was made in each 8-week-old rat 12 weeks after implantation, which also demonstrated that the model is suitable for the research of the repair of orbital defects. The results of histological analysis also showed that a large amount of new bone, including mature lamellar bone and immature woven bone formed in the orbital defect implanted with induced BMSCs/BCB composites. The immature woven bone was observed, indicating that the active new bone formation was occurring.

In general, antigen-free bovine cancellous bone is a kind of important substitute for the autogenous, allogenous grafts and synthetic material. BCB is a promising scaffold that possesses favorable characteristics for the repair of orbital defects, such as cytocompatibility for seeding cells, histocompatibility for orbit, osteoconductivity for induced BMSCs, porous structure with appropriate size for cell migration and mineral deposition, the mechanical support, and satisfactory degradation rate. BCB combined with BMSCs is a suitable tissue engineering strategy for the reconstruction of orbit defects.

On the other hand, the mechanism of BCB combined with BMSCs need to be clarified. More long-term outcomes after implantation will be investigated in further research, to determine whether BCB combined with BMSCs are capable of competing with other cell-material complexes for the reconstruction of orbital defects.

Declaration of interest The authors declare no competing financial interests. The authors alone are responsible for the content of the paper.

References

1. Iatrou I, Theologie-Lygidakis N, Angelopoulos A (2001) Use of membrane and bone grafts in the reconstruction of orbit fractures. Oral Surg Oral Med Oral Pathol Oral Radiol Endod 91:281–286

2. Heary RF, Schlenk RP, Sacchieri TA, Barone D, Brotea C (2002) Persistent iliac crest donor site pain: independent outcome assessment. Neurosurgery 50:510–517

3. Nishida J, Shimamura T (2008) Methods of reconstruction for bone defect after tumor excision: a review of alternatives. Med Sci Monit 14:RA107–RA113

4. Potter JK, Ellis E (2004) Biomaterials for reconstruction of the internal orbit. J Oral Maxillofac Surg 62:1280–1297

5. Lee S, Maronian N, Most SP, Whipple ME, McCulloch TM, Stanley RB, Farwell DG (2005) Porous high-density polyethylene

for orbital reconstruction. Arch Otolaryngol Head Neck Surg 131:446–450

6. Wang ML, Tuli R, Manner PA, Sharkey PF, Hall DJ, Tuan RS (2003) Direct and indirect induction of apoptosis in human mesenchymal stem cells in response to titanium particles. J Orthop Res 21:697–707

7. Kontio R, Suuronen R, Salonen O, Paukku P, Konttinen YT, Lindqvist C (2001) Int J Oral Maxillofac Surg 30:278–285

8. Ceonzo K, Gaynor A, Shaffer L, Kojima K, Vacanti CA, Stahl GL (2006) Polyglycolic acid-induced inflammation: role of hydrolysis and resulting complement activation. Tissue Eng 12:301–308

9. Liu Y, Ramanath HS, Wang DA (2008) Tendon tissue engineering using scaffold enhancing strategies. Trends Biotechnol 26:201–209

10. Sokolsky-Papkov M, Agashi K, Olaye A, Shakesheff K, Domb AJ (2007) Polymer carriers for drug delivery in tissue engineering. Adv Drug Deliv Rev 59:187–206

11. Yildirim M, Spiekermann H, Handt S, Edelhoff D (2001) Maxillary sinus augmentation with the xenograft Bio-Oss and autogenous intraoral bone for qualitative improvement of the implant site: a histologic and histomorphometric clinical study in humans. Int J Oral Maxillofac Implants 16:23–33

12. Young C, Sandstedt P, Skoglund A (1999) A comparative study of anorganic xenogenic bone and autogenous bone implants for bone regeneration in rabbits. Int J Oral Maxillofac Implants 14:72–76

13. Cui L, Liu B, Liu G, Zhang W, Cen L, Sun J, Yin S, Liu W, Cao Y (2007) Repair of cranial bone defects with adipose derived stem cells and coral scaffold in a canine model. Biomaterials 28:5477–5486

14. Kon E, Muraglia A, Corsi A, Bianco P, Marcacci M, Martin I, Boyde A, Ruspantini I, Chistolini P, Rocca M, Giardino R, Cancedda R, Quarto R (2000) Autologous bone marrow stromal cells loaded onto porous hydroxyapatite ceramic accelerate bone repair in criticalsize defects of sheep long bones. J Biomed Mater Res 49:328–337

15. Song C, Li G (2011) CXCR4 and matrix metalloproteinase-2 are involved in mesenchymal stromal cell homing and engraftment to tumors. Cytotherapy 13:549–561

16. Chen X, McClurg A, Zhou GQ, McCaigue M, Armstrong MA, Li G (2007) Chondrogenic differentiation alters the immunosuppressive property of bone marrow-derived mesenchymal stem cells, and the effect is partially due to the upregulated expression of B7 molecules. Stem Cells 25(2):364–370

17. Ladage D, Brixius K, Steingen C, Mehlhorn U, Schwinger RH, Bloch W, Schmidt A (2007) Mesenchymal stem cells induce endothelial activation via paracine mechanisms. Endothelium 14:53–63

18. Worth A, Mucalo M, Horne G, Bruce W, Burbidge H (2005) The evaluation of processed cancellous bovine bone as a bone graft substitute. Clin Oral Implants Res 16:379–386

19. Kneser U, Stangenberg L, Ohnolz J, Buettner O, Stern-Straeter J, Möbest D, Horch RE, Stark GB, Schaefer DJ (2006) Evaluation of processed bovine cancellous bone matrix seeded with syngenic osteoblasts in a critical size calvarial defect rat model. J Cell Mol Med 10:695–707

20. Mushipe MT, Revell P, Shelton JC (2002) Cancellous bone repair using bovine trabecular bone matrix particles. Biomaterials 23:365–370

21. Khaled EG, Saleh M, Hindocha S, Griffin M, Khan WS, Khaled EG (2011) Tissue engineering for bone production-stem cells, gene therapy and scaffolds. Open Orthop J 5(Suppl 2):289–295

22. Maniatopoulos C, Sodek J, Melcher AH (1988) Bone formation in vitro by stromal cells obtained from bone marrow of young adult rats. Cell Tissue Res 254:317–330

23. Zambuzzi WF, Oliveira RC, Pereira FL, Cestari TM, Taga R, Granjeiro JM (2006) Rat subcutaneous tissue response to macrogranular porous anorganic bovine bone graft. Braz Dent J 17:274–278

24. Han D, Li J, Guan X (2010) Ectopic osteogenesis of hBMP-2 gene-transduced human bone mesenchymal stem cells/BCB. Connect Tissue Res 51:274–281

25. He H, Cao J, Wang D, Gu B, Guo H, Liu H (2010) Gene-modified stem cells combined with rapid prototyping techniques: a novel strategy for periodontal regeneration. Stem Cell Rev 6:137–141

26. Schmitz JP, Hollinger JO (1986) The critical size defect as an experimental model for craniomandibulofacial nonunions. Clin Orthop Relat R 205:299–308

27. Schmitz JP, Schwartz Z, Hollinger JO, Boyan BD (1990) Characterization of rat calvarial nonunion defects. Acta Anat (Basel) 138:185–192

28. Yoon E, Dhar S, Chun DE, Gharibjanian NA, Evans GR (2007) In vivo osteogenic potential of human adipose-derived stem cells/ poly lactide-co-glycolic acid constructs for bone regeneration in a rat critical-sized calvarial defect model. Tissue Eng 13(3):619–627